Nuclear Instruments and Methods in Physics Research A 608 (2009) 417–423

Contents lists available at ScienceDirect

Nuclear Instruments and Methods in Physics Research A

journal homepage: www.elsevier.com/locate/nima

An LED, fiber optic, gain monitoring system for a segmented scintillator array

B.E. Bewer, R.E. Pywell *, R. Igarashi [1], W.A. Wurtz

Physics and Engineering Physics, University of Saskatchewan, 116 Science Place, Saskatoon, Saskatchewan, Canada S7N 5E2

ARTICLE INFO

Article history:
Received 20 April 2009
Received in revised form
15 July 2009
Accepted 17 July 2009
Available online 23 July 2009

Keywords:
Scintillator
Gain monitor
Fiber optics
LED

ABSTRACT

A gain monitoring system, which uses light emitting diode flashers and a fiber optic light distribution system, has been developed for use with a segmented, liquid scintillator neutron detector array. The system is designed to track neutron detector cell gains without relying on the stability of any system components. Tests show that the system is capable of tracking the gains of individual detector cells to the design accuracy of 3%.

1. Introduction

The *Blowfish* neutron detector array [1] is being used at the high intensity gamma source (HIGS) at the Duke University Free-Electron Laser Facility to make precision measurements of photoneutron cross-sections. Such measurements are needed to study fundamental properties of the nucleons and nuclear forces. *Blowfish* contains 88 detectors cells arranged in a spherical geometry that covers a solid angle of approximately $\frac{1}{4}$ of 4π steradians. Each detector cell consists of BC-505 liquid scintillator in a Lucite container attached to a phototube via a Lucite light guide. BC-505 was chosen because of its relatively benign chemical properties that allow the use of Lucite, rather than glass, cells, while having good light output efficiency at a peak wavelength of 425 nm which closely matches the response of the Photonis XP2262/B photomultiplier tubes used.

The detection of neutrons occurs primarily due to the energy deposited by recoil charged particles after a neutron interaction in the liquid scintillator. An example of such an interaction is elastic scattering from a proton. The recoil proton energy can therefore range between the energy of the neutron down to zero. The light output that ultimately reaches the phototube is related to the energy deposited by the recoil charged particles [2,3].

Therefore, the spectrum recorded by an ADC attached to a phototube for a given incident neutron energy will be something like that shown in Fig. 1. The figure shows the light output spectrum for 8.78 MeV neutrons incident on a single BC-505 cell. The energy scale is in "equivalent electron energy" units, which is the energy that an electron would have if it had the same light output as that observed from the recoiling charged particle. Mature Monte-Carlo simulations have been developed using the GEANT4 toolkit [4] that accurately predict the shape of this light output spectrum for a given experimental situation. To the GEANT4 toolkit we have added a class that, for all particle types, handles the conversion from energy deposited in the BC-505 scintillator to light output using the description given in Ref. [2]. Fig. 1 is generated by such a simulation. Ref. [2] contains examples of measured spectra compared to the GEANT4 simulation.

Since detectors are normally calibrated using a gamma ray source (by observing the Compton recoil electrons for example) the "equivalent electron energy" is the calibrated energy scale of the detector. The "gain" of a detector defines the relationship between the output of a detector, A (e.g. an ADC channel number after pedestal correction), and the equivalent electron energy deposited in the detector, E. We define the gain g by

$$E = gA. \tag{1}$$

When neutrons are incident on a detector cell a light output spectrum (such as shown in Fig. 1) will be observed. The efficiency of the detector cell is the integral of this light output spectrum divided by the number of incident neutrons. The lower bound of this integral is, in general, not zero. In a practical application it is equal to the level of a discriminator used to generate a gate for the acquisition system. Alternatively a minimum energy cut may be applied in software. Therefore, the efficiency of the detector depends strongly on the equivalent electron energy of this lower level integration limit. This in turn depends on a knowledge of the gain of the detector. The efficiency may be

* Corresponding author. Tel.: +1 306 966 6404; fax: +1 306 966 6400.
E-mail address: rob.pywell@usask.ca (R.E. Pywell).
[1] Current address: Canadian Light Source Inc., University of Saskatchewan, 101 Perimeter Road, Saskatoon, Saskatchewan, Canada S7N 0X4.

0168-9002/$ - see front matter © 2009 Elsevier B.V. All rights reserved.
doi:10.1016/j.nima.2009.07.021

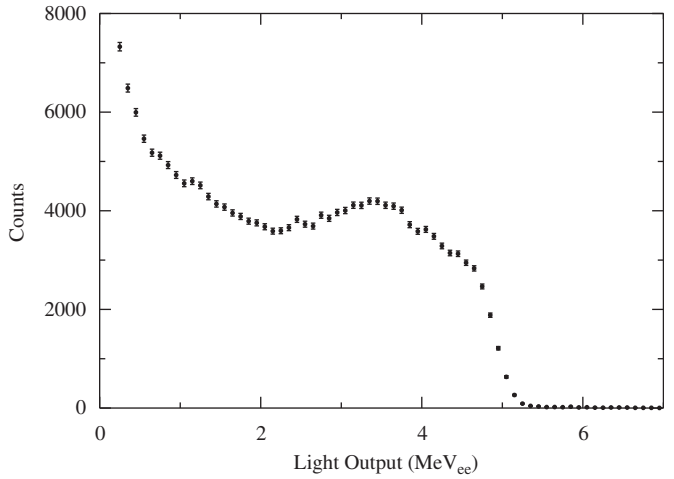

Fig. 1. The spectrum from a BC-505 scintillator cell when 8.78-MeV neutrons are incident on it. The spectrum was generated by a GEANT4 simulation.

determined experimentally for certain specific situations but in general we must make use of the GEANT4 simulation to predict the efficiency for more complex experimental arrangements. In either case an accurate value for the detector gain at the time of measurement is needed.

The required accuracy of the gain depends on the accuracy of the detector efficiency needed, as well as the neutron energy and the detector threshold used. For the measurements we propose for *Blowfish* we are striving for efficiencies to be known to 2% or better. This is not difficult for high neutron energies but for low neutron energies and/or high threshold energies the needed gain accuracy becomes more stringent. As examples, for a 6 MeV neutron with a detector threshold of 500 keV$_{ee}$ the gain needs to be known to better than 8% to achieve a 2% accuracy in efficiency, while for a 1 MeV neutron with a 100 keV$_{ee}$ threshold the gain needs to be known to within about 4%. Therefore, to provide sufficient accuracy for the measurement we plan for *Blowfish*, we aimed to develop a system that would allow us to determine the gain of a particular cell to within about 3% at any time during an experiment.

The gain may be measured at a particular time using a radioactive source with a convenient known energy gamma ray. However there are many things that may cause the gain to drift over the period of a measurement (e.g. over the course of a day). Drifts in the phototube supply voltage or temperature and count rate effects in the phototube itself are prime examples. Changes in other active components of the electronics may also cause gain changes. Therefore, a method of continuously monitoring the gain as a function of time is of vital importance for high precision measurements.

Many experimenters have made use of light flashers distributed to detector elements by fiber optics to monitor detector gains. A xenon flasher system has proved useful for slow time constant NaI detectors (e.g. the Boston University NaI, BUNI, detector [5]). More recently light emitting diode (LED) flashers have been used (e.g. Ref. [6]). These LED systems have taken great care to ensure the stability of the LED and light distribution system since they rely on that stability.

We have chosen to use an LED fiber optic based system because the light pulses can be made to simulate the time constants of the BC-505 detector elements. However we have designed a system that does not rely on the stability of the LED system, but tracks it with a monitor detector after the fashion used by the BUNI detector [5].

2. Gain tracking principles

The concept of the gain monitoring system is illustrated in Fig. 2. A pulser will fire a single LED whose light will be captured by a fiber optic bundle. Individual fibers in the bundle take the light to the neutron detector cells in *Blowfish* (only one is shown in the figure). As well a fiber in the same bundle takes light to a separate monitor detector. A radioactive source is also present near the monitor detector.

The data acquisition system will allow the recording of several different types of events:

1. A "normal" event: When a particle is incident on a cell the ADC value for that cell is recorded.
2. When the pulser fires: The ADC value for each cell, which results from the LED light reaching it, is recorded. As well, the ADC value for the monitor detector, which results from the LED light reaching it, is recorded.
3. When a gamma ray from the radioactive source interacts with the monitor detector the ADC value from it is recorded.

There are two types of data taking runs relevant to this discussion. A "calibration" run is when a radioactive source with a convenient energy is placed near the *Blowfish* cells so that their gains may be determined. During a "data taking" run, for example with the accelerator beam on, there is no radioactive source near the *Blowfish* cells, so no direct measure of the cell gains is possible. All types of events listed above are recorded for both types of runs and separate histograms are accumulated for each different event type in each run.

During a calibration run a feature from the radioactive source near the *Blowfish* cells with light output E_S is observed to be at ADC channel A_{Si} in cell i. The gain for cell i is then determined by

$$g_i = E_S/A_{Si}. \quad (2)$$

At the same time data are recorded from the LED flasher. If an amount of light L is produced by the LED, and a certain fraction x_i of it reaches cell i, then the peak due to the LED flasher will appear in channel

$$A_{Fi} = x_i L/g_i. \quad (3)$$

If a feature from the radioactive source near the monitor detector with light output E_M is observed to be at ADC channel A_m then the monitor gain is determined by

$$g_m = E_M/A_m. \quad (4)$$

If the fraction of the LED light L reaching the monitor detector is x_m, then the peak due to the LED flasher in the monitor histogram

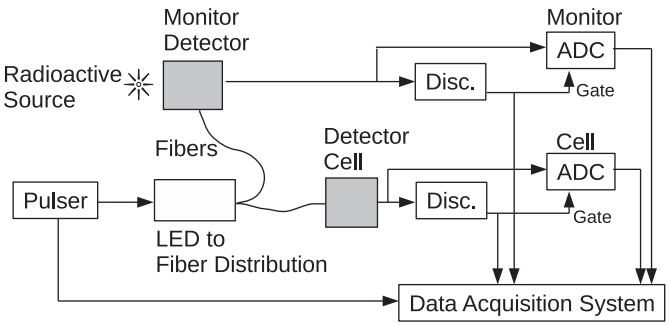

Fig. 2. Conceptual schematic of the gain monitoring system. When the pulser fires the data acquisition system will record ADC values from the detector cells as well as from the monitor detector. In addition, the data acquisition system will record ADC values from the monitor detector when a signal caused by the radioactive source is present and the pulser is not present.

will appear in channel

$$A_{Fm} = x_m L/g_m. \quad (5)$$

All the quantities here are known or measured except L, x_i and x_m. Combining Eqs. (3) and (5) the following ratio for each cell can be calculated:

$$R_i = \frac{x_i}{x_m} = \frac{g_i}{g_m}\frac{A_{Fi}}{A_{Fm}}. \quad (6)$$

During a later data taking run the light produced by the LED may have changed, the gains of the cells may have changed, and the gain of the monitor detector may have changed. We denote these changed quantities by L', g_i' and $g_{m'}$ respectively. If the source feature in the monitor spectrum appears at channel $A_{m'}$ then the monitor gain can be determined from

$$g_{m'} = E_M/A_{m'}. \quad (7)$$

We allow the fraction of the LED light reaching cell i to now be x_i' and the fraction of the LED light reaching the monitor detector to now be $x_{m'}$. Then the flasher peak will appear in the cell spectrum at channel

$$A_{Fi}' = x_i' L'/g_i' \quad (8)$$

and in the monitor spectrum at channel

$$A_{Fm'} = x_{m'} L'/g_{m'}. \quad (9)$$

Combining Eqs. (8) and (9) we solve for the required cell gain

$$g_i' = g_{m'}\frac{A_{Fm'}}{A_{Fi}'}\frac{x_i'}{x_{m'}} = g_{m'}\frac{A_{Fm'}}{A_{Fi}'}R_i' \quad (10)$$

where $R_i' = x_i'/x_{m'}$.

We now make the assumption that $R_i' = R_i$. This is a justifiable assumption provided there are no serious mechanical changes between the two runs that could change the light transport efficiency through the fibers going to the *Blowfish* cells or to the monitor detector. The required cell gain in the data taking run is then given by

$$g_i' = g_{m'} R_i \frac{A_{Fm'}}{A_{Fi}'}. \quad (11)$$

Therefore, provided the assumption of $R_i' = R_i$ is valid, the gain at any time may be calculated without the need to assume absolute stability of the gain monitoring components. Nevertheless, in the design of the gain monitoring system reported here, efforts were made to ensure maximum stability where ever possible. Additional details of the design may be found in Ref. [7].

3. Gain monitor design

The light source must be capable of fast pulsing and have an output in the blue region of the spectrum so as to mimic as close as possible the scintillator output. The NSPB series LEDs from Nichia Corporation fitted these criteria and several were chosen for further testing. The peak emission wavelength of these LEDs is 465 nm, which is in the range of the BC-505 light emission spectrum. The LEDs produce light in a forward cone with a given opening angle. Because we want the light to enter a fairly large bundle of fibers (about 13 mm in diameter) the uniformity of the light in the cone was tested. This was done by allowing the light to shine on a piece of paper. A CCD camera on the opposite side of the paper was used to collect an image. This process was used because the LED was too bright for a direct exposure to the CCD camera. These tests showed that some LED models did not have a sufficiently uniform light intensity profile. The NSPB310 LED was selected because it has a light intensity that varied smoothly with angle. If a fiber bundle was a few centimeters away from this LED the intensity change from fiber to fiber would be small. This LED also had a fairly linear relationship between driving voltage and light output.

A BNC 555-8c bench-top pulser was used to drive the LED. This model has eight output channels which can be independently adjusted. Pulse widths as short 10 ns can be achieved with pulse amplitudes between 1 and 6 V. On the 20 ns pulse width setting, for example, the pulse has a rise time of 12.1 ns (10–90%) and a fall time of 5.5 ns (90–10%) with a FWHM of 21.3 ns. The output pulse amplitudes showed only slow drifts with time, generally less than 0.1% per hour.

The NSPB310 LED, coupled with the BNC 555 pulser, was tested to determine the pulse to pulse light output stability of the combination. A photomultiplier was used to detect the light pulses. As expected the stability depended on the driving voltage and the pulse width. For short pulse widths the full width half maximum (FWHM) of the light output intensity was unacceptably large. A pulse width of 20 ns was chosen as being a good compromise. It is sufficiently short to mimic the scintillator output while having a FWHM below 10% for a wide range of pulser voltages. This FWHM was sufficiently small to allow accurate peak fitting to pulser spectra during operation. The FWHM as a function of pulser voltage for a pulse width of 20 ns is shown in Fig. 3.

Light transmission was accomplished using Eska GH2001 step index plastic fibers made by Mitsubishi Rayon. The fibers needed to be able to transmit visible light and needed to be flexible with consistent light transmission after repeated bending. Large core plastic fibers provide the best collection of incident light. For this reason a step index fiber was chosen because at the time of construction large core plastic fibers were not available with a graded index profile. The chosen fibers have a core with refractive index 1.49 and the cladding has refractive index 1.40. These fibers have a core diameter of 0.48 mm, an overall diameter of 0.5 mm, and a light transmission loss of 0.15 dB/m.

Each LED supplied light to a bundle of 30 fibers. Four LED/bundle combinations provided enough fibers to feed light to the 88 detectors in *Blowfish* and to a monitor detector associated with each bundle. In addition each bundle contained seven spare fibers. Each fiber was 8 m long which resulted in an acceptable 25% light loss along a fiber. At one end, where the LED light enters, the fiber bundle is held together with an aluminum sheath. This sheath is rigidly clamped into a light tight aluminum housing which also contained the LED. An illustration of this

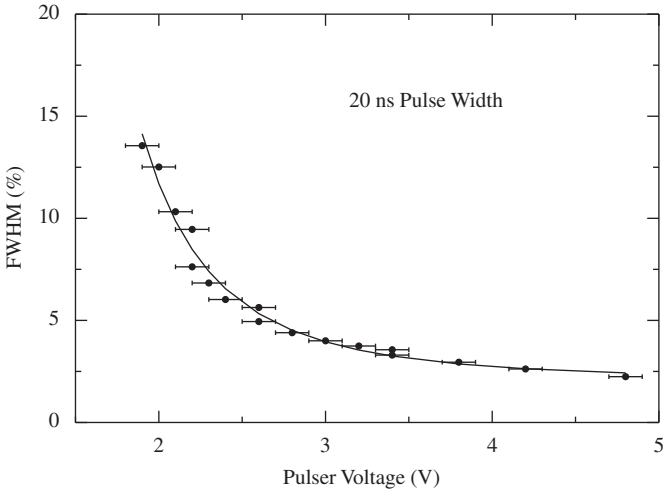

Fig. 3. The measured FWHM of the light output of the NSPB310 LED as a function of pulser voltage for a pulse width of 20 ns. The line is a fit to the data points.

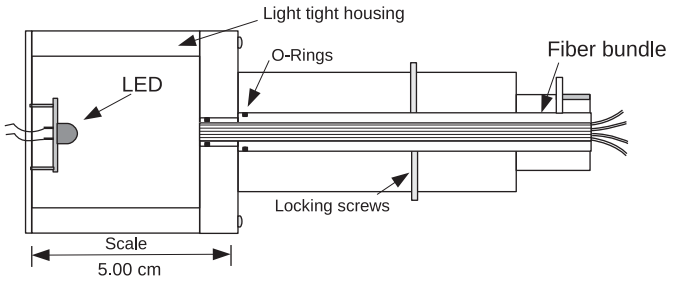

Fig. 4. A schematic of the light tight LED housing which mates to the end of a bundle of optical fibers.

arrangement is shown in Fig. 4. Because better resolution was obtained by running the BNC 555 pulser at a relatively high voltage it was found necessary to attenuate the light entering a fiber bundle. This was accomplished by introducing an approximate neutral density filter between the LED and the bundle. These filters are disks cut from a translucent plastic sheet. The ends of all fibers are crimped into an ST bayonet connector for quick removal and attachment to the BC-505 detectors and the monitor detectors.

The monitor detectors need to be compact while dense enough to allow the full energy peak from a radioactive gamma source to be observed. A cerium doped Gd_2SiO_5 crystal (GSO) was chosen as it has a relatively high specific gravity of 6.71 which allowed the full energy peak from the 0.662 MeV gamma ray from a ^{137}Cs source to be observable in a small crystal (of about 1.2 cm in diameter). GSO also has an emission spectrum similar to that from BC-505, and therefore also similar to the light from the LED. In addition GSO has a relatively short decay time constant of 0.056 μs, which simplifies the detector electronics. GEANT simulations were used to choose a suitable size of GSO crystal that could be coupled to a small phototube while having a sufficient count rate, of about 1 Hz, from a weak radioactive source. A ^{137}Cs source was chosen because of its relatively long half life and the simplicity of its gamma ray spectrum. A cylindrical GSO crystal of diameter 12.7 and 12.7 mm long was found to be sufficiently large. This crystal was coupled to a Hamamatsu R1450 phototube which has a diameter of 19 mm and an active area width of 15 mm. This was accomplished by placing the GSO crystal in an acrylic sheath with an outside diameter equal to that of the PMT. The crystal and sheath were optically coupled to the PMT with silicone rubber and placed in a plastic detector tube. The acrylic sheath also allowed easy coupling of the LED fiber to the detector. Four GSO detector assemblies were mounted in a box near a single ^{137}Cs source.

The BC-505 detectors need to operate over a wide range of gains to detect different neutron energies. After a gain change the pulse height from the BNC 555 pulser can be adjusted to keep the pulser peak in a useful part of the neutron detector ADC spectra. However the gain of the GSO monitor detectors cannot be adjusted since it is necessary to keep the ^{137}Cs source peak within a usable range. Therefore, it is sometimes necessary to adjust the LED light reaching the monitor detectors by adjusting the attenuation of light. Thus a set of optical attenuators were constructed. These attenuators are just short segments of optical fiber which make use of the natural attenuation of light at the ST connector. An adjustment of the attenuation factor can be accomplished by marking the end of the fiber in an attenuator segment with a felt tip pen to reduce the light transmission.

Delivery of the LED light to the BC-505 detector cells was accomplished by inserting a section of fiber optic cable into a flat-bottomed hole drilled into the Lucite light guide. The cable is held in place by epoxy binding the cable sheath to the light guide. The cable runs alongside the PMT to an ST adapter which is attached to the detector base next to the high voltage and signal connectors.

It is desired to minimize motion of the fiber optic cables running from the LED boxes to the detectors. Therefore, since *Blowfish* is designed to be rotated during operation, the LED boxes were mounted on the *Blowfish* arms so there is no relative motion between the LED boxes and the detectors. Because the fiber optic cables are all the same length it is sometimes necessary to coil up unnecessary cable length. Such coils are protected in plastic tubing which also prevents kinking of the fiber optic cable. In the initial setup of the system the GSO monitor detectors were mounted on a non-rotating part of the *Blowfish* stand. This did allow motion of the fiber optic cable going from the LED boxes to the monitor detectors. The effect of this will be discussed in Section 4.2.

4. Performance tests

After installation a set of system tests were performed where deliberate changes were made to gain monitor components to determine the overall effectiveness of the system in tracking the

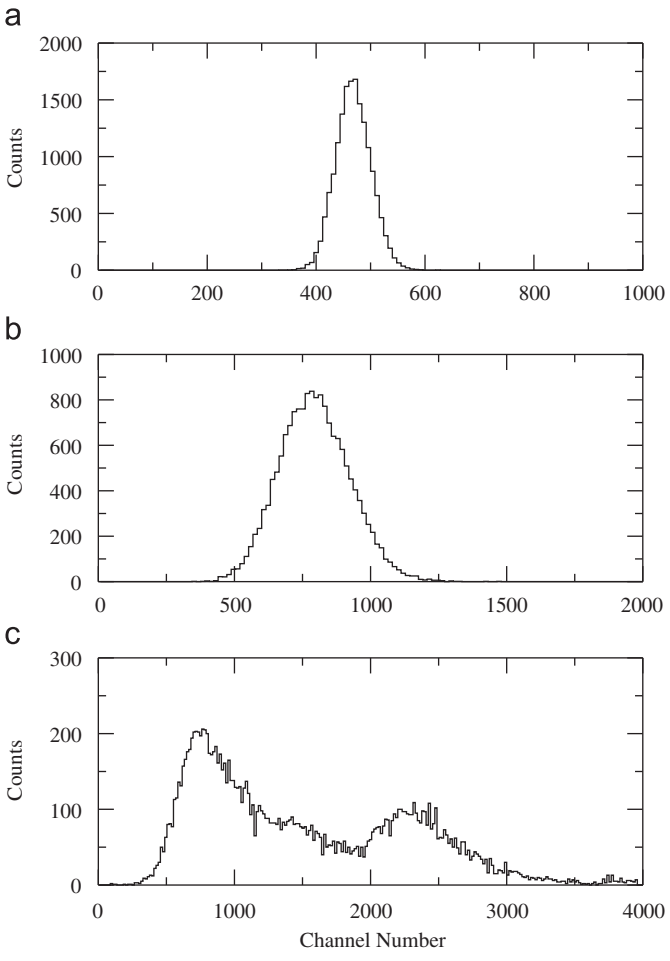

Fig. 5. Examples of the spectra relevant to the gain monitoring system from a single data taking run. A typical flasher peak in a *Blowfish* cell is shown in (a). A typical flasher peak in a GSO monitor detector is shown in (b). A typical spectrum from the ^{137}Cs source in a GSO monitor detector is shown in (c), with the full-energy peak at around channel 2300. Note that the flasher resolution in (b) is poorer than in (a) because, as described in Section 3, some light attenuation was used in the fiber going to the GSO detector in order to keep the flasher peak on scale in the ADC.

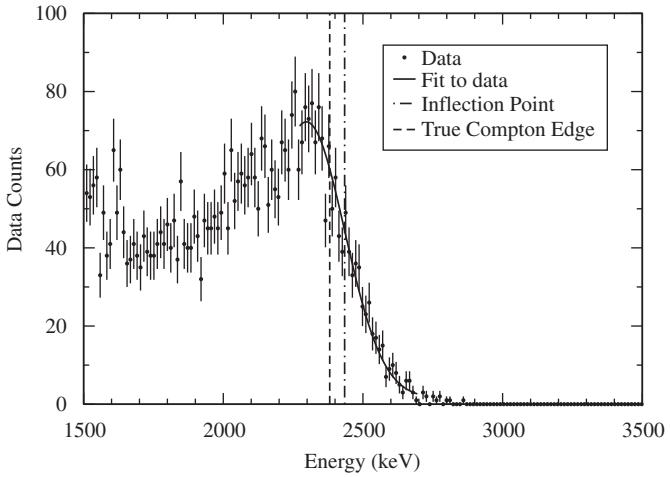

Fig. 6. An example of fitting to the Compton edge in a BC-505 cell. The data points with error bars shows the Compton edge for the 2.614 MeV gamma ray from a thorium source. The solid line shows the fit to the data used to find the inflection point which is shown by the vertical dot-dashed line. The energy scale has been calibrated so that the position of the inflection point matches that determined from a simulation. The vertical dashed line shows the energy of the Compton edge.

Blowfish cell gains. Later more stringent tests under actual data taking conditions were performed. Both will be summarized here.

Examples of the spectra relevant to the flasher monitoring system are shown in Fig. 5. The cell and monitor detector flasher peaks were each fitted with a simple Gaussian distribution to determine the centroid. The centroid of the full energy peak due to the ^{137}Cs source in the GSO monitor spectrum is found by fitting it with a Gaussian, along with a Gaussian tail background.

The cell gains were determined by observing the location of the Compton edge in the light output spectrum for each cell when a radioactive gamma ray source was present. Several gamma ray sources are used for these measurements. We have made use of the 4.430 MeV gamma ray from an AmBe source, the 0.969 and 2.614 MeV gamma rays from a ^{232}Th source, and even the 1.461 MeV gamma ray from ^{40}K present in the room background has been useful. The Compton edge was located by finding the inflection point in a curve fitted to the endpoint of the light output spectrum. The fitting function used is one side of a Gaussian curve. An example of this fit is shown in Fig. 6 for the Compton edge from the 2.614 MeV gamma ray from a thorium source. Using the GEANT4 simulation it was found that this inflection point was always a little higher in energy than the true Compton energy, and that the difference was independent of gamma ray energy. Therefore, the inflection point energy, as predicted by the simulation for the particular BC-505 cell configuration in *Blowfish*, was used as the known energy feature to calculate the gains using Eq. (2).

4.1. System tests

Initial testing of the gain monitoring system followed a standard procedure for each test. First the gain of all the cells was determined using a radioactive source. From the monitor and flasher information taken during this initial calibration run a set of R_i values can be calculated. It should be noted that since there are four monitor detectors in the final system the subscript m in Eq. (6) (and other equations in Section 2) runs from 1 to 4, while the subscript i runs from 1 to 88. In calculating the quantities in Section 2 it is important to use the monitor m that is in the same fiber bundle that goes to a particular cell i.

After the R_i values have been determined a deliberate change in some element of the system was made. The changed gain for each cell was again measured using the radioactive source. As well, the changed gain was calculated using the flasher information from Eq. (11) using the R_i values from the first run. The calculated and measured gains were then compared.

To get an overall sense of how well Eq. (11) predicted the gains for all cells we calculate the following two quantities. If the measured gain for cell i is $g_{i,meas}$ and the calculated gain is $g_{i,calc}$, we define a "fractional gain error" in percent by

$$e_i = \left|\frac{g_{i,meas} - g_{i,calc}}{g_{i,meas}}\right| \times 100\%. \tag{12}$$

The "mean gain error" for all cells is then

$$\bar{e} = \frac{1}{88}\sum_{i=1}^{88} e_i \tag{13}$$

and a "gain error standard deviation" σ_e in percent is defined by

$$\sigma_e^2 = \frac{1}{88}\sum_{i=1}^{88}(e_i - \bar{e})^2. \tag{14}$$

The "mean gain error" gives a sense of how well the gain tracking system is able to predict the true gain averaged over all 88 cells. The "gain error standard deviation" gives a sense of how the gain error for individual cells deviate from the "mean gain error." The results from several system tests are listed in Table 1.

The first test involved deliberately changing the LED light output. This was accomplished by changing the pulser voltage by 50 mV. This change, of about 1.7%, is actually quite large since, as noted above, the pulser amplitude has been observed to have drifts of less than 0.1%. The second pair of tests involved deliberately changing the gain of the GSO monitor detector. This was accomplished by changing the GSO PMT high voltages by 10 and 20 V. The third pair of tests involved deliberately changing the gain of all the *Blowfish* cells. This was accomplished by changing the cell PMT high voltages by 10 and 20 V. The results in Table 1 show that the gain monitoring system was, on average, able track the *Blowfish* cell gains with an accuracy of at least about 1.5%.

4.2. Tests under data taking conditions

Under normal experiment running conditions it is only possible to do a limited number of cell gain calibration runs using a radioactive source. During a measurement at HIGS covering a 10 day period during September and October 2008, calibration runs were performed usually at the beginning and end of each day's data

Table 1
The results from gain monitor system tests where deliberate changes to gain monitor components were made.

Test	Mean gain error, $\bar{e}$ (%)	Gain error standard deviation, σ_e (%)	Mean cell gain change (%)
50 mV change in LED pulser voltage	0.49	0.31	0
10 V change in GSO high voltages	0.43	0.34	0
20 V change in GSO high voltages	0.59	0.48	0
10 V change in cell high voltages	0.84	0.67	6.0
20 V change in cell high voltages	0.83	0.66	12.1

As described in the text, the values "mean gain error" and "gain error standard deviation" quantify how well the gain monitoring system is able to predict the correct gain after a change was made.

taking. The Compton edge from the 4.430 MeV gamma ray from an AmBe source was most commonly used as the calibration feature for these measurements. Using these calibration runs it is possible to check the accuracy of the gain monitoring system.

We show two examples. In the first example we compare calibration run 832 with run 866 taken 24 h later. In Fig. 7 the top frame shows the ratio between the R_i for each cell derived from run 866 divided by the R_i value from run 832. The cells are grouped according to which fiber bundle it belongs. Each fiber bundle is driven by a different LED and one fiber from each bundle goes to a different monitor detector. It can be seen that there is excellent agreement between the R_i values derived from the two runs. This confirms the assumption that the R_i values do not change, at least for this example.

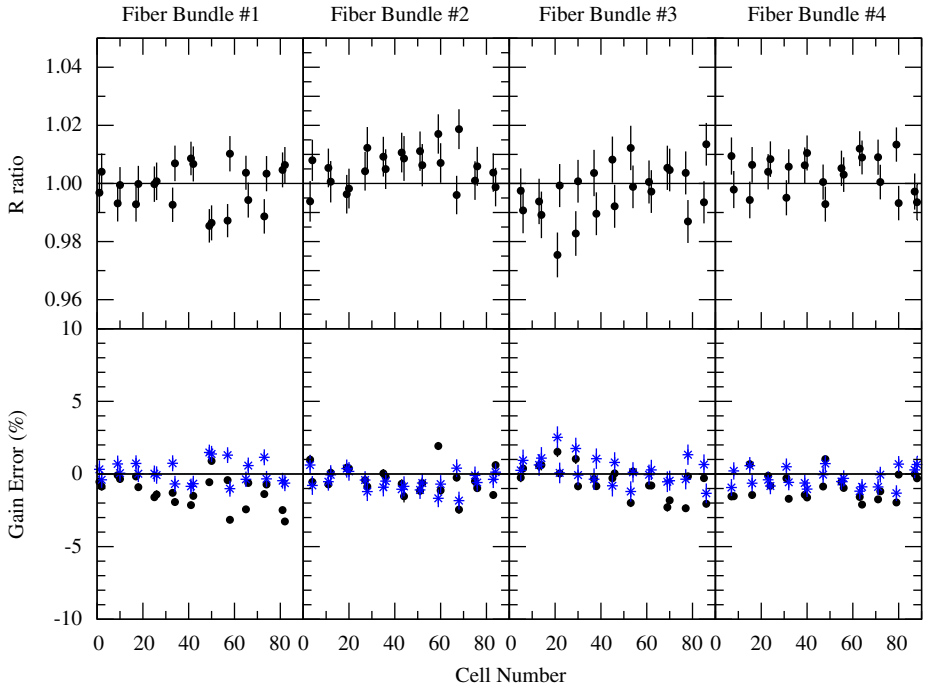

Fig. 7. A comparison between calibration runs 832 and 866 that were taken 24 h apart. The top frame shows the ratio between the R_i for each cell derived from run 866 divided by the R_i value from run 832. The bottom frame shows the gain change between the two runs. The solid circles show the percentage change in gain for each cell derived from run 832 compared to the gain derived from run 866. The stars show the percentage difference between the calculated gain for run 866, derived using the gain monitoring information, and the actual measured gain from run 866. Additional explanation is given in the text.

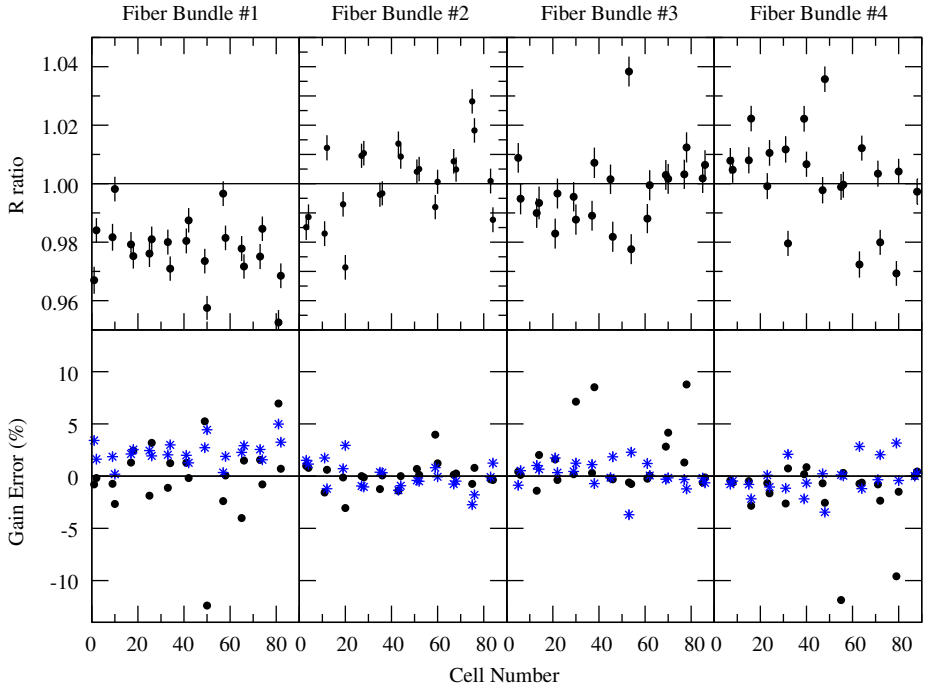

Fig. 8. A comparison between calibration runs 944 and 980 that were taken 13.5 h apart. The explanation of the symbols is the same as for Fig. 7.

The bottom frame in Fig. 7 shows the gain change between the two runs. The solid circles show the percentage change in gain for each cell derived from run 832 compared to the gain derived from run 866. The stars show the percentage difference between the calculated gain for run 866 and the actual measured gain from run 866. The gain is calculated using the R_i values derived from the earlier run 832 and the flasher information from run 866. It can be seen that the calculated gains are within 2% of the actual gain. This gives us confidence that we can calculate correctly the gains for runs between the two calibration runs 832 and 866. In practice the average of the two R_i values from the two calibration runs will be used when calculating the gains for the intervening runs which further reduces the uncertainty in the calculated gains. In this example there were no large gain changes in the cells, so the good agreement is perhaps to be expected.

In the second example we compare calibration run 944 with run 980 taken 13.5 h later. In Fig. 8 we see that there is generally good agreement between the R_i values for the cells in fiber bundles 2–4. However for the cells in fiber bundle 1 there appears to be a systematic shift in the R_i values. This suggests that there was a change in the light transport efficiency x_m along the fiber going from the LED to the monitor detector. This comes about because the *Blowfish* array was rotated during the time period between the two runs. The monitor detectors are mounted on the non-rotating frame of the detector array so the fiber going from the LED to the monitor detector does have to move when the *Blowfish* array is rotated. Apparently, in this case, this movement caused a change in the light transport efficiency along the fiber to monitor detector 1. This effect can be avoided in several ways. Calibration runs can be done before and after any array rotation so that such changes can be tracked. Alternatively we can avoid such changes altogether by mounting the monitor detector on the rotating part of *Blowfish* so that there is no relative movement of any of the fiber optic cables.

The bottom frame in Fig. 8 shows the gain change between the two runs and the difference between the calculated and actual gain for run 980. It can be seen that, at least for the cells in fiber bundles 2–4, the calculated gains are within about 3% of the actual gain. This is true even for cells where there have been up to 15% changes in the actual gain between the two runs. It can also be seen that the calculated gains for the cells in fiber bundle 1 are systematically in error due to the systematic shift in R_i values for that bundle.

5. Conclusion

We have developed a gain monitoring system based on an LED flasher where the light is distributed to individual cells by fiber optic cables. The light output from the LED is monitored by a scintillator whose gain is in turn monitored by a feature in a radioactive source. Therefore, the operation of the gain monitoring system does not depend on the stability of any of its components. The system has been shown to be able to predict the gain of an individual cell to be within about 3% under actual experimental conditions, thus meeting the design criteria.

Acknowledgment

The financial assistance of the Natural Science and Engineering Research Council of Canada is gratefully acknowledged.

References

[1] B.D. Sawatzky, Ph.D. Dissertation, University of Virginia, 2005 (Unpublished).
[2] R.E. Pywell, B.D. Sawatzky, J. Ives, N.R. Kolb, R. Igarashi, W.A. Wurtz, Nucl. Instr. and Meth. A 565 (2006) 725.
[3] G.V. O'Rielly, N.R. Kolb, R.E. Pywell, Nucl. Instr. and Meth. A 368 (1996) 745.
[4] GEANT4 Collaboration, Nucl. Instr. and Meth. A 503 (2003) 250; GEANT4 Collaboration, IEEE Trans. Nucl. Sci. NS-53 (2006) 270.
[5] E.L. Hallin, et al., Phys. Rev. C 48 (1993) 1497.
[6] M.H.R. Khan, et al., Nucl. Instr. and Meth. A 413 (1998) 201.
[7] B.E. Bewer, M.Sc. Thesis, University of Saskatchewan, 2005 (Unpublished).